buildings

MDPI

Article

Study of the Moisture Behavior of Natural Composites and Their Possible Influence on the Interior Microclimate with Green Elements

Jitka Peterková [1,*], Jiří Zach [1], Vítězslav Novák [1], Azra Korjenic [2], Jolan Oskar Schabauer [2] and Abdulah Sulejmanovski [2]

[1] Institute of Technology of Building Materials and Components, Faculty of Civil Engineering, Brno University of Technology, Veveří 331/95, 602 00 Brno, Czech Republic; jiri.zach@vut.cz (J.Z.); vitezslav.novak1@vut.cz (V.N.)

[2] Institute of Material Technology, Building Physics, and Building Ecology, Faculty of Civil and Environmental Engineering, TU Wien, Karlsplatz 13, 1040 Vienna, Austria; azra.korjenic@tuwien.ac.at (A.K.); jolan.schabauer@tuwien.ac.at (J.O.S.); abdulah.sulejmanovski@tuwien.ac.at (A.S.)

* Correspondence: jitka.peterkova@vut.cz; Tel.: +420-541147524

Abstract

The indoor environment of buildings is of fundamental importance for the health of people and other living organisms residing in them. From this perspective, key factors include indoor temperature, relative humidity and the concentration of CO_2 or other pollutants. These healthy indoor conditions are typically maintained through functional heating and ventilation systems. However, in the case of indoor humidity, increasing moisture levels when they are low can be relatively challenging. There are more energy-efficient solutions that can be combined with ventilation systems. These include, for example, placing plants and green walls in the interior, which have a significant impact not only on microclimatic and acoustic conditions of the interior, but also on the overall psychological well-being of occupants. Green elements contribute to the effective regulation of CO_2 and certain other harmful substances within the indoor environment. Another possible solution involves the use of sorption-active materials in the form of cladding panels—elements capable of functioning as indoor regulators, i.e., absorbing moisture and releasing it back into the indoor environment when necessary. This study investigates the moisture behavior of natural composites based on montmorillonite clay and straw fibers, as well as their possible integration with green elements to create healthy indoor conditions for their inhabitants. The developed clay composite can be classified as water and steam absorption class WSIII according to DIN 18948—the moisture buffering capacity value was 152.73 g/m^2 after 12 h. Based on the research results, it can be stated that these composites could serve as interior cladding elements in synergy with green elements (*Chlorophytum comosum*, *Epipremnum aureum*), ideally regulating the indoor microclimatic conditions, especially as an effective solution for short-term humidity changes. The maximum difference in relative humidity between the reference testing chamber (without green elements and clay plates) and the chamber containing plant *Chlorophytum comosum* and three clay composite plates was 23.04%.

Keywords: natural composite; sorption; moisture buffering value; green wall; microclimate of interior

Academic Editor: Paulo Santos

Received: 1 October 2025
Revised: 14 November 2025
Accepted: 18 November 2025
Published: 24 November 2025

Citation: Peterková, J.; Zach, J.; Novák, V.; Korjenic, A.; Schabauer, J.O.; Sulejmanovski, A. Study of the Moisture Behavior of Natural Composites and Their Possible Influence on the Interior Microclimate with Green Elements. *Buildings* **2025**, *15*, 4230. https://doi.org/10.3390/buildings15234230

1. Introduction

The quality of the indoor environment of buildings is a key factor influencing the health of their inhabitants. Currently, there is a trend towards the construction of passive or near-zero energy buildings, which exhibit very low thermal energy losses in both heating and cooling. However, a frequent problem is the indoor microclimate, because natural air exchange is limited in these buildings. Ventilation is typically achieved mechanically with recuperation. As a result, problems frequently arise due to inappropriate levels of indoor relative humidity—particularly when humidity is not regulated together with heating via air-conditioning units, which is expensive and energy intensive. Air-conditioning units are often used to adjust the indoor environment (especially for summer cooling), yet their high energy demand makes them an unsuitable solution from an environmental point of view. Their use to improve indoor environments leads to health problems of occupants, such as the drying of mucous membranes, which negatively affects the overall health of residents [1].

As shown by numerous studies, the indoor microclimate can be significantly stabilized by using natural materials with a high sorption activity, such as unfired ceramics, clay plasters and other materials [2,3]. Clay remains a widely used building material and a raw material for given building materials. Today, about a third of the Earth's population lives in clay houses, predominantly in developing countries, where clay is an easily accessible raw material for various building products [4]. Although this material was largely replaced by concrete and other modern materials in the 20th century, society is increasingly returning to clay construction, which represents healthy housing with a low impact on the environment.

Clay acts as a natural humidity regulator, significantly improving indoor comfort. The effect is determined by the content and structure of given clay minerals in the soil. Clay soils consist of a mixture of clay (plastic) minerals (kaolinite, montmorillonite, illite, chlorite) and non-clay (non-plastic) minerals (quartz, micas, feldspar, limestone). Clay minerals are a group of layered aluminosilicates (phyllosilicates characterized by their fine-grained structure, high specific surface area and their ability to adsorb water and ions). Their basic crystal structure consists of a combination of tetrahedral (SiO_4) and octahedral (AlO_6 or MgO_6) layers. These layers are combined into basic building units arranged as 1:1 (e.g., kaolinite) or 2:1 (e.g., montmorillonite and illite). The differences in structure among clay minerals determine their ability to bind water, expand, exchange cations and influence the transport properties of materials [5–7]. The formation of clay minerals is associated with the chemical weathering of primary silicate minerals, especially feldspars and micas. The process occurs in the presence of water, carbon dioxide and weak acids, which disrupt the original structure of the minerals and lead to the formation of secondary phases. The resulting clay minerals, such as montmorillonite, illite and kaolinite, are stable compounds with varying degrees of crystallinity and chemical composition [8–10]. In terms of the sorption behavior, the presence of hydroxyl groups, negative surface charge and exchangeable cations play a significant role. While surfaces with hydroxyl groups show a high affinity for water due to the formation of hydrogen bonds, purely silicate surfaces are relatively hydrophobic. Minerals with an expandable structure (e.g., montmorillonite) allow the entry of water molecules and ions into their interlayers, which leads to structural expansion. This phenomenon is crucial for the water retention and swelling ability [5–7,11].

Clay minerals include the following groups: kaolinite ($Al_2O_3 \cdot 2SiO_2 \cdot 2H_2O$), montmorillonite ($Al_2O_3 \cdot 4SiO_2 \cdot nH_2O$) and illite ($nK_2O \cdot Al_2O_3 \cdot 3SiO_2 \cdot nH_2O$) (see Figure 1). The kaolinite group consists of the two-layer clay minerals kaolinite ($Al_2O_3 \cdot 2SiO_2 \cdot 2H_2O$) and halloysite ($Al_2O_3 \cdot 2SiO_2 \cdot 2H_2O \cdot 2H_2O$). These minerals can be two- or three-layered, with layer thicknesses, composed of Si-O tetrahedra and Al-(OH) octahedra, typically ranging from 0.7 to 2 nm. In illite, potassium cations K^+ are located between the three layers. The

preferred ionic radius K tightly binds the individual triple layers, preventing welling. In contrast, montmorillonite contains absorbed cations (e.g., Ca^{2+}, Na^{+}, Mg^{2+}) between the triple layer, surrounded by layers of water, which promotes swelling and increases the distance between the triple layers to an average of 1.4 nm [12].

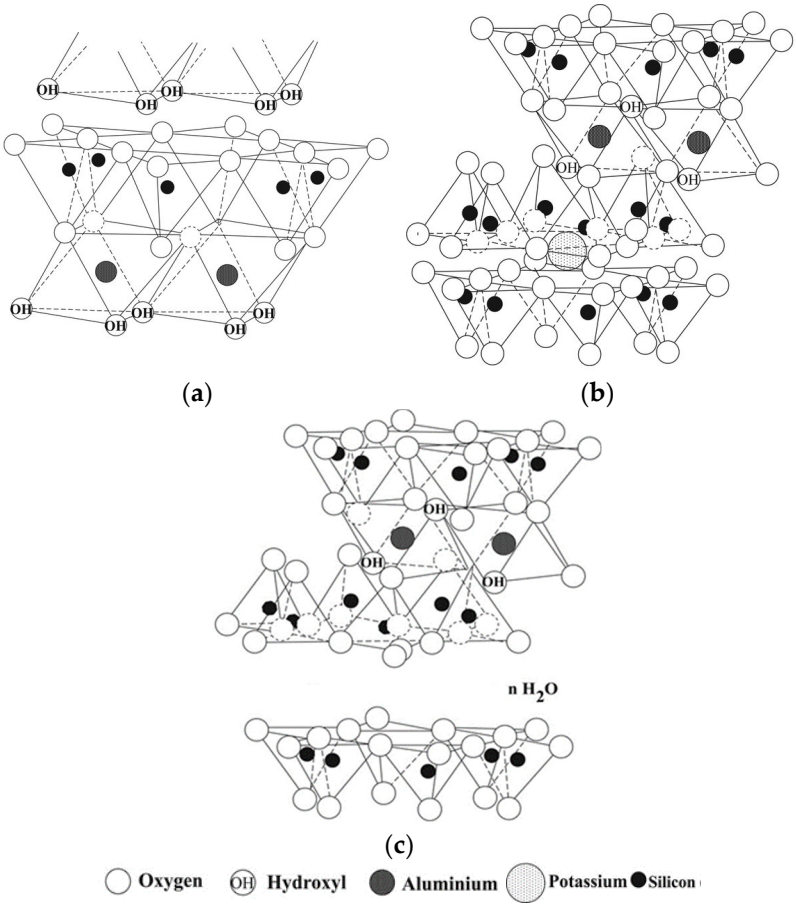

Figure 1. Crystallographic description of kaolinite (**a**), illite (**b**) and montmorillonite (**c**) [13].

1.1. The Principle of Water Binding to Clay Minerals

The binding of water to clay minerals is the result of a combination of physicochemical processes, with the efficiency depending on the crystal chemistry of the given mineral, the type of its surfaces, the presence of exchangeable ions and external conditions such as the relative humidity and temperature. Water can bind to clays on the surface (adsorption) or in the interlayer space (intercalation) or be retained by capillary action in the pores between aggregated particles [6,14]. On the surface of clay minerals, water binds through hydrogen bonds, mainly to –OH groups (e.g., aluminol surfaces of the Al–OH type). This primary bond allows the formation of monolayer sorption. Surfaces rich in Si–O–Si groups (e.g., siloxane surfaces) are weakly polar and exhibit a low affinity for water. The ability to bind water is therefore significantly higher on hydroxylated surfaces than on purely silicate surfaces [5,15].

At a higher relative humidity, a multilayer structure of water molecules forms above the surface. These layers are stabilized not only by hydrogen bonds between water molecules, but also by dispersion (van der Waals) forces, which are necessary for maintaining structures higher than one monomolecular layer. Without taking these interactions into account, it is impossible to correctly model the sorption energetics or spatial arrangement of water. In minerals with an expandable structure (especially montmorillonite), water intercalates into the interlayers, where it binds to exchangeable cations (e.g., Na^{+}, Ca^{2+}).

These ions create hydration shells, thereby increasing the distance between the layers and causing structural swelling of the mineral. This type of bonding is partially reversible and depends on the chemical composition of the clay, the type of ion present and its hydration energy. Water may also bind only physically as a result of capillary absorption in the pores [6,11,14,16].

The influence of clay minerals on the characteristics of final construction products containing clay soil has been described by numerous authors. Portuguese scientists Lima et al. monitored the behavior of three types of plasters containing different proportions of clay minerals—kaolinite, illite and montmorillonite—and confirmed that the mineralogical composition has a significant influence on the plaster properties such as water vapor adsorption, drying shrinkage and mechanical and thermal insulation properties. In their study, illitic clay soil was evaluated as the most suitable raw material for the use in plasters [17]. Research by Altmäe et al. also confirmed significant differences in eight different clay–sand plasters, studied in terms of sorption properties and water vapor permeability [18].

Due to this moisture behavior of clay soils, the negative phenomenon of shrinkage can occur to varying degrees depending on the proportion of individual clay minerals. When water evaporates, dimensional changes in the material can lead to shrinkage cracks. This effect can be addressed by adding plant fibers or aggregates. Numerous studies have demonstrated that adding such fibers effectively reduces crack formation [19–22]. Meglio et al. investigated the effect of reinforcing adobe bricks with natural fiber. They found that hemp reinforcement, in specific configurations, effectively limits shrinkage and enhances the compressive strength of the adobe bricks, demonstrating a viable option for sustainable construction materials [23]. Natural fibers can also improve the mechanical properties and resistance of clay composites, as shown by Hurtado-Figueroa et al. [24], who tested rice straw, and Koutouse et al. [25], who examined the effect of barley straw and date palm fibers. In general, it can be stated that, by incorporating natural fibers and aggregates into the clay soil matrix, it is possible to modify and improve selected properties of composites, e.g., reducing water absorption to prevent shrinkage and improving mechanical properties. The results of research on the hygrothermal behavior of composites composed of clay and olive fibers show that the use of these bio composites can achieve significant energy savings related to indoor humidification and drying processes [26,27]. However, there remains a lack of fundamental research focused on the humidity behavior, hygroscopic properties and durability of clay–fiber composites [28].

In addition to moisture adsorption, clay materials can also effectively adsorb air pollutants, which is highly favorable for improving the indoor microclimate of buildings. This ability has been described by numerous researchers. This is due to the porous structure, large specific surface area, excellent cation exchange capacity and the presence of Brönsted and Lewis acids in clay minerals [29]. Darling et al. demonstrated the ability of clay materials (paints) to reduce ozone concentrations indoors [30–32]. Hu et al. [33] and Kausor et al. [34] described the ability of montmorillonite to adsorb heavy metals and organic substances.

1.2. Healthy Building Environment

A healthy indoor environment can be effectively influenced already during the building design stage through the proper design and composition of the building structure (including the materials used) and the optimization of air flow and ventilation [35,36]. Furthermore, the incorporation of indoor green elements, green facades or sorption-active materials can help achieve these goals. The properties and functions of sorption-active clay-based materials have already been described above. Another effective approach involves the use of green facades and green interior elements, which positively influence a healthy indoor

microclimate, improve acoustic conditions, absorb dust particles and other harmful substances and contribute to the occupants' psychological well-being [37–39]. Improvements in acoustic properties have been described by Davis, M. J. M. et al. and Azkorra, Z. et al. from the perspective of sound absorption properties [40,41] and Peterková et al. from the perspective of reverberation time [42]. Van Renterghem, T. presented a comprehensive study on the positive effect of vegetation on noise perception [43]. These acoustic and environmental benefits are significantly influenced by the appropriate selection of the green wall system, the choice of suitable plants and the selection of the appropriate substrate [44]. This issue is addressed from a normative point of view by, for example, ÖNORM L 1133 [44]. Green plants are characterized by the process of photosynthesis, a set of chemical reactions in which the energy of sunlight is absorbed and used to convert simple inorganic compounds into organic substances, with oxygen produced as a by-product. The process of photosynthesis can be expressed by the following simplified equation:

$$6CO_2 + 12\ H_2O \rightarrow C_6H_{12}O_6 + 6O_2 + 6H_2O \quad (1)$$

From an energetic point of view, photosynthesis increases the internal energy: ΔH° = +2870 kJ/mol. Therefore, photosynthesis plays an important role in mitigating excess heat during the summer, both indoors and outdoors in buildings [45].

The aim of the research work carried out in cooperation between Brno University of Technology and Technical University Vienna is to study the possibility of stabilizing the internal environment of buildings using a combination of sorption-active materials/elements based on clay composites and green elements in order to keep the internal humidity within 40–60% throughout the day. The main aim is to find suitable materials that allow the humidity to be regulated in the range of 35–55% (at 23 °C indoor temperature) using their sorption activity. A suitable material should exhibit the steepest possible sorption curve in the range of 35–55% relative humidity and demonstrate the greatest difference in humidity between its limiting states (sorption capacity), enabling it to adsorb moisture at a high indoor relative humidity and release moisture at a low relative humidity. This article presents the results of work in which, based on previous research [12], montmorillonite clay-based raw materials and easily available straw fibers were selected as potential ecological materials for bio composites with excellent sorption/desorption characteristics. These composites can be further combined with green/active elements and conventional measures such as ventilation or targeted indoor air exchange and treatment. The scientific contribution of this research is primarily focused on the influence of the mineralogical composition of clay on the moisture behavior of natural composites, as previously detailed [12]. Furthermore, the novelty of this work is the combination of clay-based bio composites with green elements to regulate indoor humidity, an area largely unexplored.

2. Raw Materials

Based on previous research results, locally available raw materials with a low environmental impact (low carbon footprint) were selected for the development of sorption-active composite materials. Clay (LB Minerals, Horní Bříza, Czech Republic) with a high content of montmorillonite from LB Minerals, whose mining sites are located in the Czech Republic, was chosen as the binder. The material was selected due to its low carbon footprint and its ability to create a composite structure with a good ratio of sorption and mechanical properties. Clay generally provides the coating of the reinforcing skeleton formed by the filler and serves the primary function of controlling humidity in a given environment. The filler was selected as a readily available natural agricultural fiber on the market—wheat straw (ISO-STROH, Mitterfeld, Austria), which exhibits favorable moisture capacity, low

bulk density and relatively good thermal insulation properties. The straw was supplied in a dust-free and sorted form.

The basic characterization and determination of selected properties were performed on the input raw materials (clay, straw fibers); see Figure 2 (see Part 2 below).

(**A**) (**B**)

Figure 2. Photography of used raw materials; clay with organic filler ((**A**)—clay based on montmorillonite; (**B**)—straw).

Based on the initial experiments [12], the optimal ratio of input raw materials to produce test specimens was proposed in the volume ratio of 30:70—binder (clay)/filler (natural fibers—straw). This ratio ensured a balance between an open pore structure and a sufficient mechanical resistance of the test specimens. The specimens were prepared by incorporating the filler into the clay slurry, with each raw material being dosed by weight. The mixture was homogenized manually. The thoroughly mixed material was then placed in special bottomless molds positioned on a fine grid to ensure sufficient air flow during drying. The specimens were dried until their weight stabilized under laboratory conditions (23 °C and RH 50%). These specimens were subjected to selected tests for the subsequent verification of their properties, especially the possible use as sorption-active materials for adjusting the indoor microclimatic conditions (see below). The specific composition of the mixture, converted into weight doses for 1 dm^3, is given in Table 1 below.

Table 1. Mixture composition.

Composition of Mixture	**Amount per 1 dm^3 [g]**		
	Filler	**Soil**	**Water**
	62	261	328

3. Methodology

The methodology of the work was divided into several parts. The first part focused on the characterization of selected properties of the raw materials. The second part involved studying the plastic–clay dough to determine the optimal water content for the subsequent preparation of hardened clay samples. The third part was devoted to the properties of hard-

ened clay samples, including composites based on clay and straw fibers, by determining selected physical and mechanical properties. For each test, at least three specimens were subjected to the testing of selected properties according to normative procedures, and the results were reported as the average values. At the final stage, a semi-scale experiment was conducted. The produced composite samples were placed in plexiglass boxes with a volume of 1 m^3, together with green plants intended for green walls, to investigate moisture behavior and the potential for regulating indoor humidity.

3.1. Input Raw Materials

Selected properties were determined on the input raw materials (clay, straw):

(a) Clay

- *Chemical analysis* was determined according to EN ISO 12677 [46] with the X-ray fluorescence (XRF) method. The sample was dried, ground and sieved through a 0.063 mm sieve. Next, the sample was melted with a flux (a mixture of lithium tetraborate, lithium metaborate and lithium iodide) in a ratio of 1:10. The resulting pearl was then subjected to XRF in a PANalytical Axios analyzer (Malvern Panalytical Ltd., Malvern, United Kingdom).
- *Microscopic analysis* used a scanning electron microscope TESCAN MIRA3 XMU (Tescan Group, a.s., Brno, Czech Republic) for depicting individual minerals.
- *X-ray diffraction analysis* used a PANalytical Empyrean device (Malvern Panalytical Ltd., Malvern, UK) for the determination of qualitative composition.
- *Determination of fines by flotation*: A dried clay test sample weighing 200 g (m_0) was placed in water for 1 h to allow it to float. The sample was then placed on a sieve with a mesh size of 0.063 mm and washed with water until the water ran clear. After sieving, the clay retained on the sieve was dried in a drying oven at 105 °C, until its weight stabilized, and then weighed (m_1). For the content of fines smaller than 0.063 mm, $R_{0.063}$ was determined using to the following relationship:

$$R_{0.063} = (m_0 - m_1) \times 100/m_0 \quad (2)$$

(b) Straw

- *The determination of loose density* was performed according to EN 1097-3 [47] on samples of straw with a volume of 1 dm^3. For this measurement, straw was conditioned at +23 °C and a relative humidity of 50%. The bulk density was calculated according to Equation (3), where m is the mass of the sample material and V is the volume of the test container:

$$\rho = m/V \quad (3)$$

- *The determination of the grain size* of straw particles was performed through sieve analysis according to EN 933 [48]. A standard set of sieves was used, consisting of sieves with mesh sizes of 125; 63; 31.5; 16; 8; 4; 2; 1; 0.5; 0.25; 0.125; and 0.063 mm. From the measured data, the percentage drop of each individual sieve was calculated and the grain size curves were constructed.

3.2. Plastic Dough

A plastic dough was prepared from the clay in order to determine the following:

- *Optimal moisture*, w_{opt}, was determined according to CSN 72 1074 [49], using a Pfefferkorn apparatus (Anderen Ltd., Stoke-on-Trent, UK); see Figure 3A. A 500 g sample was used to prepare two malleable doughs with different moisture contents by gradually adding water. These doughs were stored for 24 h in a desiccator, the lower part of

which was filled with water. From each dough, five test cylinders were prepared using a metal mold, with a diameter of (33 ± 0.5) mm and a height of (40 ± 0.5) mm. The optimal deformation ratio for the test dough was determined to be d = 0.6.

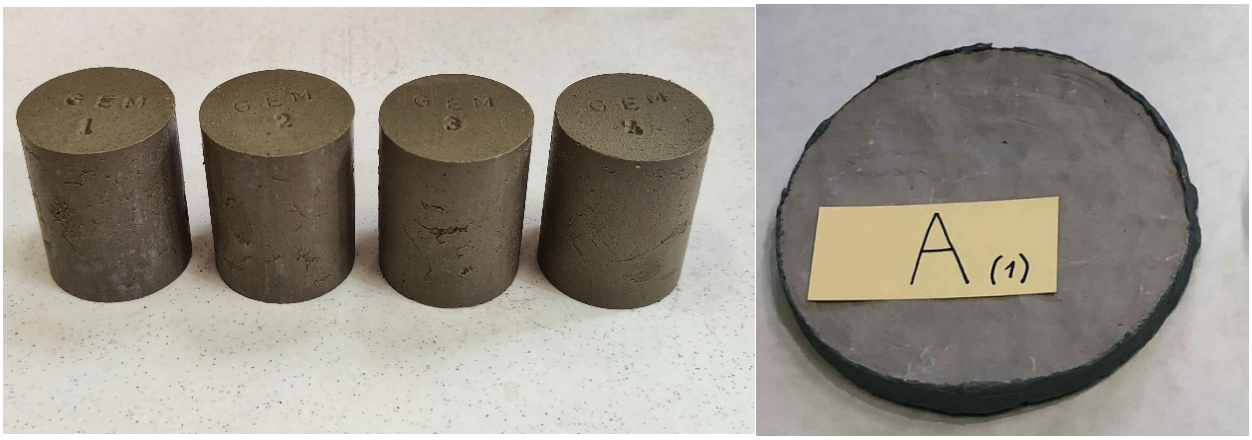

(**A**) (**B**)

Figure 3. Testing samples for determining (**A**) optimal moisture and (**B**) moisture buffering capacity.

The optimal moisture content was determined according to the following relationship (4), where w_1 is the moisture content of the first (harder sample) sample in %, w_2 is the moisture content of the second (more plastic) sample in %, d_1 is the deformation ratio of the first sample, d_2 is the deformation ratio of the second sample and d = 0.6:

$$w_{opt} = w_1 + [(w_2 - w_1) \times (d - d_1)/(d_2 - d_1)] \quad (4)$$

- *Sensitivity to drying* was determined according to Bigot *SDB* and according to CSN 721073 [50]. The measurement was performed on 100 × 50 × 20 mm samples, which were manufactured with optimal humidity and subsequently dried gradually. The change in dimensions and humidity over time was continuously recorded. In the end, the samples were dried at a temperature of 110 °C, and the critical humidity w_{kb} was determined from the measured values. The Bigot sensitivity to drying coefficient (SDB) was determined according to the following relationship (5):

$$SDB = (w_a - w_{kb})/w_{kb} \quad (5)$$

3.3. Hardened Clay Samples

For hardened clay samples, the following were then determined:

- *The determination of bulk density*, ρ_v, was performed according to CSN 72 2603 and EN ISO 29470 [51,52], both in the fresh and the hardened/air-dry state (23 °C, 50% RH).
- *Mechanical properties* (flexural tensile strength and compressive strength) were determined according to CSN 72 1565-7 [53] and EN ISO 29469 [54]. The determination of the compressive strength σ_m was carried out according to EN ISO 29469, through a procedure suitable for measuring the strength of highly porous materials before their critical deformations are reached. A test specimen with a thickness d was placed between the fixed pressing plates of the testing device and loaded at a rate of 0.1 d min^{-1}. The initial pressure acting on the specimen was 250 ± 10 Pa, with the compressive force applied perpendicular to the parallel surface. The maximum compressive force transmitted by the test specimen was then determined from the working diagram. If the maximum force value corresponded to a deformation of less than 10%, the compressive strength would be calculated. If the test specimens did not fail before

reaching 10% deformation, the compressive stress at 10% deformation was calculated. The compressive strength was expressed according to (6), where F_m is the maximum compressive force and A_0 is the cross-sectional area of the test specimen:

$$\sigma_m = \left(F_m \times 10^3\right) / A_0 \quad (6)$$

The tensile strength, σ_{po}, was tested on five dried test beams measuring 20 × 20 × 120 mm. The evaluation was carried out according to the following Equation (7), where F is the force at the moment of failure, l is the distance of supports, b is the width of the cross-section of the test specimen and h is the height of the cross-section of the test specimen:

$$\sigma_{po} = (1.5\ F \times l) / \left(b \times h^2\right) \quad (7)$$

- *Sorption properties* were determined according to EN ISO 12571 [55] at 23 °C, at different relative humidity levels: 33, 53, 75, 85 and 98% RH. Sorption/desorption curves were compiled based on the weight changes in specimens after reaching equilibrium humidity, starting from either dry or saturated states.
- *The moisture buffering capacity* for pure clay was measured using a modified methodology based on DIN 18948 [56], NORDIC TEST methodology [57] and ISO 24 353 [58]. Due to the nature of the clay sample, circular samples with a diameter of 180 mm and a thickness of 15 mm were used (see Figure 3B). Testing conditions were adjusted to simulate indoor environmental conditions, as the target function of the material was to serve as a sorption-active element in buildings. Humidity cycling was performed in a climatic chamber at a temperature of +23 °C in the range of relative humidity levels of 35% and 65%. According to DIN 18948, the amount of moisture absorbed/released by the material in g/m^2, denoted G(t), was determined at given time intervals. Subsequently, the moisture buffering capacity, MBV, was determined as the ratio of the amount of moisture that the material absorbs or releases over a given time, G(t), and the difference in relative humidity in the environment to which the material is exposed, in % (ΔRH).
- *Shrinkage* for pure clay: This measurement was performed on circular samples conditioned under laboratory conditions (23 °C, 50% RH) to determine the moisture buffering capacity, with the sample's areal dimensions measured prior to testing. These dimensions were measured immediately after the test specimens were prepared and again after drying under laboratory conditions. Shrinkage was calculated based on the changes in the dimensions of the specimens.

3.4. Composites

Composites were produced by first mixing clay with a specified amount of water and adding straw, followed by a thorough homogenization. Plate-shaped samples were produced, and selected properties were determined on test specimens in the same manner as hardened clay test samples.

The following tests were performed on the test samples after drying and weight stabilization (23 °C, 50% RH):

- *The determination of bulk density*, ρ_v, was performed according to CSN 72 2603 and EN ISO 29470 [51,52], both in the fresh and hardened/air-dry state (23 °C, 50% RH).
- *The determination of compressive strength*, σ_m, compressive stress at 10% strain was performed according to EN ISO 29469 [54].
- *The determination of the thermal conductivity*, λ, was performed using a non-stationary method in the state of practical humidity (23 °C/50%RH).

- *The determination of the sound absorption coefficient*, α, was performed according to ISO 10 534-1 [59], a method based on the creation of standing waves in an interference tube. From the measured values, single-digit values of the weighted sound absorption coefficient α_w [-] were determined based on EN ISO 11 654 [60]. Based on these values, the test specimens were subsequently classified into sound absorption classes.
- *The determination of sorption properties* according to EN ISO 12571 [55] was carried out in the same way as for hardened clay test specimens.
- *Determination of moisture buffering capacity*: The measurement was performed (similarly to clay) using a modified method based on DIN 18948 [56], NORDIC TEST [57] and ISO 24 353 [58]. Humidity cycling was performed in a climatic chamber at a temperature of +23 °C in the range of relative humidity of 35 and 65%. The evaluation was performed from the perspective of all three tested methodologies, while the desorption dependence was also determined for composite samples (according to ISO 24 353).
- *Shrinkage* for composites was measured in the same way as for hardened clay test specimens, according to CSN 72 1073 [50].

3.5. Small-Scale Experiment

A small-scale experiment was designed to investigate the interaction between plant transpiration, substrate evaporation and the moisture-regulating behavior of clay panels (bio composites—clay with straw). The aim was to evaluate the extent to which clay panels are able to buffer high humidity levels under semi-real conditions and release them again when humidity decreases. The aim was to investigate whether the use of clay panels in indoor spaces, combined with plants, has a measurable effect on relative humidity.

For this purpose, two identically configured, airtight test boxes made of Plexiglas, with an internal volume of 1 m^3 each, were compared (see Figure 4). During the test period, one box contained only a plant with a substrate, while the second box also contained a defined number of clay panels with dimensions 100 × 280 mm on an aluminum frame. Both boxes were positioned in front of a north-facing window. To avoid the influence of direct and indirect sunlight and temperature-related distortion, the window was fitted with a frosted glass film. The room temperature was set between 22 °C and 24 °C using an air conditioner.

The temperature and relative humidity were continuously recorded in both chambers at two-minute intervals using two HygroClip2 devices (brand: Rotronic; Bassersdorf, Switzerland), which had been calibrated beforehand in Rotronic hygrogen (brand: Rotronic; Bassersdorf, Switzerland). The air was exchanged daily at 10:30 a.m. using regulated compressed air, whereby the air fed in could be used at the same time to specifically reduce the humidity, thus lowering the relative humidity to 50%. An integrated pressure relief valve enabled the controlled discharge of excess air when the dry compressed air was blown in.

- Plant and substrate selection: Based on preliminary tests [61], two indoor plant species were selected for the experiments: *Chlorophytum comosum* (spider plant) and *Epipremnum aureum* (ivy arum). The leaf area of both plant species was measured photometrically using the smartphone app "LeafByte". *C. comosum* and *E. aureum* were cut to approx. 800 cm^2 so that two individuals of the same species had a comparable leaf area.

A mixture of 90 vol.% clay granules (manufacturer: Seramis; Mogendorf, Germany) and 10 vol.% vermiculite was used as the plant substrate. Both substrates were sieved to a grain size of 4–7 mm using DIN ISO 3310-1 [62] and ISO 565 [63] analysis sieves.

Figure 4. Experimental setup.

This resulted in two independent test series with different plants. The plants were planted three weeks before the start of the experiment in PVC pots with a diameter of 12 cm and a height of 10.5 cm. Each pot was filled with 550 mL of the respective substrate.

- Test procedure: At the start of the test run, the plants were watered to a volumetric water content of 20% in the substrate. Depending on the test, one, two or three clay plates were taken from the climate chamber, measured gravimetrically and placed on a corresponding holder inside one of the two test boxes. The clay plates were pre-conditioned in a climate chamber Feutron-model 3623-21 (Feutron Klimasimulation GmbH, Langenwetzendorf, Germany) in accordance with DIN 18948 at 23 °C and 50% relative humidity [56]. Both boxes were then sealed, and data recording was started.

The following day, at 10:30 a.m., the relative humidity in the boxes was abruptly reduced to 50% using compressed air. This marked the start of the actual measurement phase. Over the next six days, the humidity was lowered again to 50% at 10:30 a.m. each day. After completing the series of measurements, the chamber was opened, and the experiment was ended. Both the clay plates and the pots with substrate and plants were weighed. Three series of measurements were carried out for each plant species, each with one, two and three clay plates.

Since the measurements were carried out successively in two chambers only, always in the chamber with the plant and in the chamber with the plant and plate, it was necessary to exclude side effects, especially small temperature fluctuations (despite the measures described above leading to their elimination). Therefore, data analysis was performed using the ANOVA test on the data obtained from the chamber without clay, which represented the reference conditions. This test was intended to confirm or exclude the hypothesis that the measurement is influenced by side effects, which is crucial for further reproducibility of the obtained results.

4. Results and Discussion

This section presents the results of the measurements performed on both the input raw materials, hardened clay samples and the composites (clay with straw) made from

them. At least three test samples were subjected to a testing of the selected properties with regard to normative procedures, and the evaluation was then performed as the average value from these measurements.

4.1. Characteristics of Input Raw Materials

A test sample of the selected montmorillonite clay was subjected to a determination of key properties. The chemical composition of the clay is shown in Table 2 below.

Table 2. Chemical composition of clay [%].

Chemical Compound	SiO_2	Al_2O_3	TiO_2	Fe_2O_3	CaO	MgO	K_2O	Na_2O
Percentage amount	56.57	19.80	1.40	12.49	1.39	3.21	2.70	0.36

As expected, there were mainly silicon and aluminum oxides identified, with smaller amounts of iron, magnesium, potassium and calcium oxide. The mineralogical composition is visible in the XRD analysis (Figure 5), where mainly the minerals kaolinite, illite, montmorillonite, quartz and micas were detected.

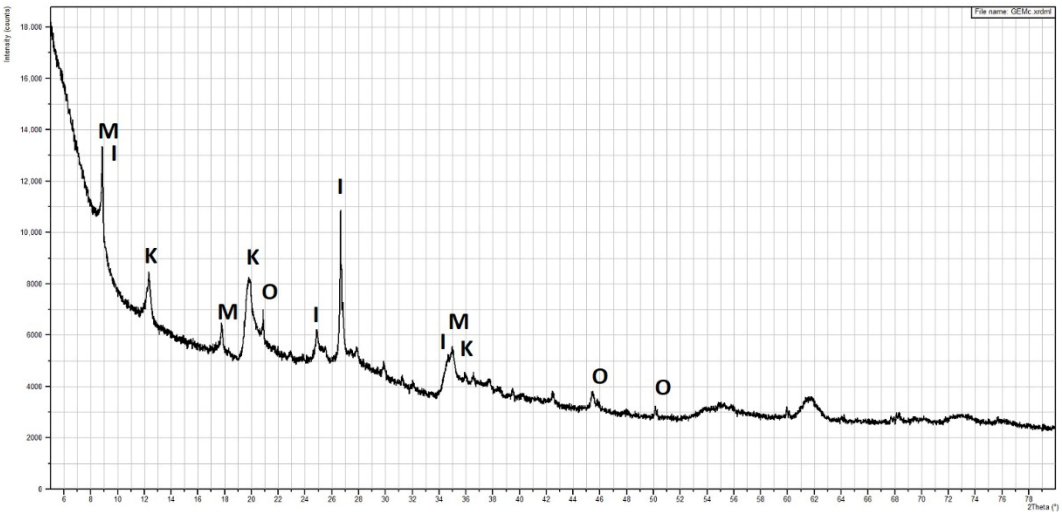

Figure 5. X-ray diffraction analysis of clay (K—kaolinite, I—illite, M—montmorillonite, O—quartz).

Scanning electron microscopic (SEM) analysis of the pure clay confirmed the presence of individual kaolinite, montmorillonite and illite minerals in the layers. An example of an SEM image of the clay is shown in Figure 6, where the presence of kaolinite, montmorillonite and a fine structure of illite is evident. The image shows a distinct laminar and foliated microstructure of clay. A complex system of layered flakes and plate-like aggregates can be observed, which is typical for minerals of the kaolinite and illite group. These aggregates are characterized by relatively compact plates with well-developed surfaces and occasionally sharper edges. Locally, an exfoliation and loosening of the layers occurs, which is a characteristic manifestation of the presence of smectites, i.e., montmorillonite. This structure is particularly evident in the form of finely wavy edges, irregularly flaking fragments and micropores forming between the individual lamellae.

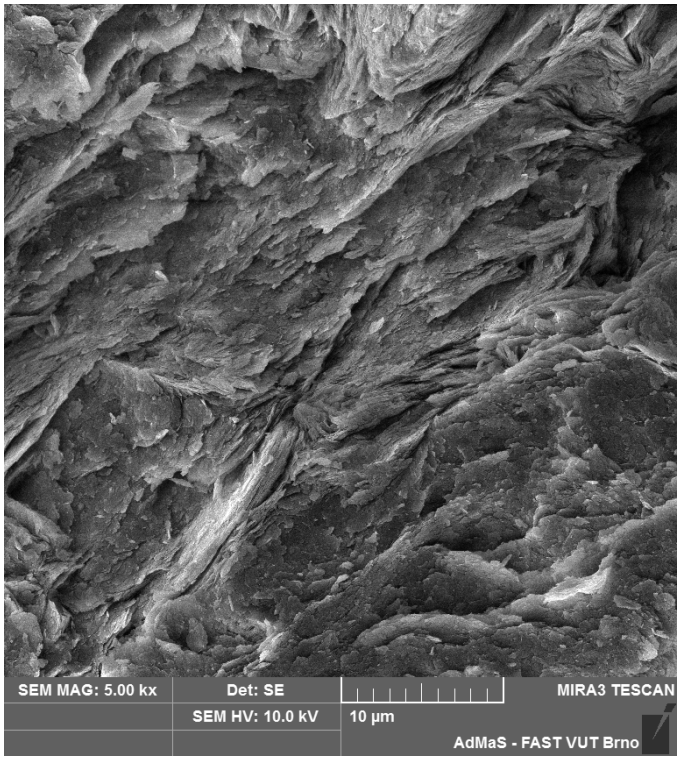

Figure 6. Image of clay from a scanning electron microscope (SEM).

The proportion of fine particles ($R_{0.063}$) in the pure clay, characterized by an increased content of montmorillonite, was equal to 20.96%.

The loose density and grain size curves were determined on three samples of straw. Straw had a loose density of 80.86 ± 3.63 kg/m^3. The results of the sieve analysis are presented in Figure 7, showing that approximately 15% of the straw particles are smaller than 1 mm.

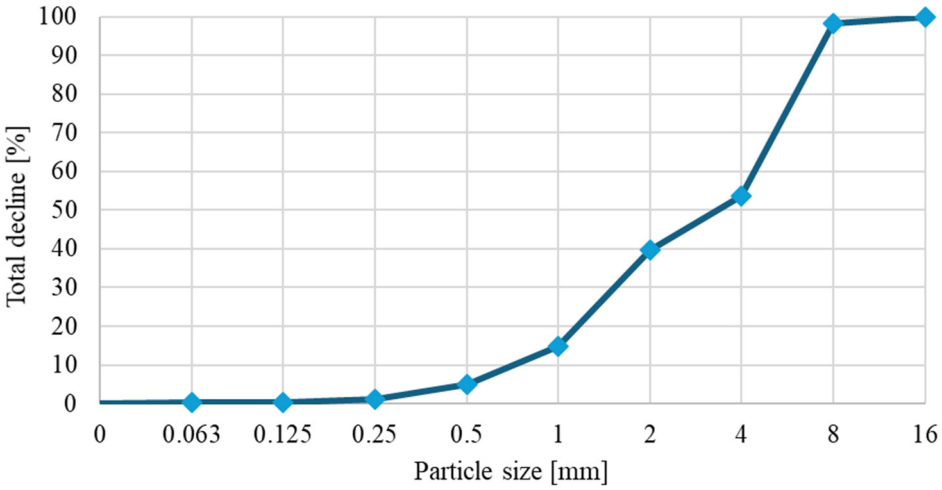

Figure 7. Sieve analysis of straw.

4.2. Characteristics of Plastic Dought

The optimum moisture content for the plastic dough of montmorillonite clay was determined as w_{opt} 50.58 ± 0.06% and SDB 2.89 ± 0.16. Based on these values, it can be concluded that this clay is specified as very sensitive to drying.

4.3. Characteristics of Hardened Clay Samples

Three test samples of specified dimensions were subjected to bulk density measurements in the fresh state and under standard laboratory conditions (23 °C/50%RH). The average value of bulk density in the fresh state was 1800 ± 5.16 kg/m^3; the bulk density in the dry state was 1580 ± 4.27 kg/m^3.

Mechanical properties were determined on five hardened test specimens of given dimensions of pure clay. The average value of the flexural tensile strength was 0.91 ± 0.04 MPa, and the average value of the compressive strength was 8.47 ± 0.18 MPa.

The shrinkage of pure montmorillonite clay was tested for five test specimens. The average value with the standard deviation was 14.81 ± 0.44%.

The determination of sorption properties and moisture buffering capacity was performed on three hardened clay samples.

The evaluation of sorption properties and moisture buffering capacity is presented for comparison in Section 3.4, where the results for both pure clay and the composite (clay + straw) are presented.

Table 3 below provides an overview of the average property values determined for hardened clays.

Table 3. Evaluation of selected properties of hardened clay samples.

Property	Average Value with Standard Deviation	Unit
Density—fresh state	1800 ± 5.16	kg/m^3
Density—hardened state	1580 ± 4.27	kg/m^3
Compressive strength	8.47 ± 0.18	MPa
Flexural tensile strength	0.91 ± 0.04	MPa
Shrinkage (linear)	14.81 ± 0.44	%

4.4. Overview of Results Determined on Composites

Three test samples of specified dimensions were subjected to bulk density measurements in the fresh state and under standard laboratory conditions (23 °C/50% RH). Additional measurements were performed on the samples after conditioning, including the determination of the thermal conductivity, sound absorption coefficient and mechanical properties—the tension at 10% deformation. These tests were conducted primarily to assess their potential use as interior cladding elements. The results are given in Table 4. Based on these results, it can be concluded that the average values obtained for the basic physical, mechanical and thermal insulation and acoustic properties are sufficient for their use as cladding elements intended for indoor humidity regulation. The measured thermal conductivity of the composite material (λ = 0.1277 ± 0.0002 W/(m·K)) indicates significantly improved thermal insulation properties compared to conventional interior cladding materials. According to the available literature, the thermal conductivity of gypsum plasterboards is typically around 0.25 W/(m·K), while conventional lime–cement plasters exhibit values in the range of 0.7–1.0 W/(m·K) [64,65]. In terms of acoustic performance, an improvement is also evident—the weighted sound absorption coefficient α_w = 0.45 corresponds to class A according to EN ISO 11654, whereas standard gypsum boards usually reach α_w values of approximately 0.10–0.15, corresponding to class E [60]. These results demonstrate that the composite material exhibits a combination of favorable thermal insulation and sound absorption characteristics, making it suitable for interior applications aimed at enhancing both thermal comfort and acoustic quality.

Table 4. Evaluation of selected properties.

Property	Average Value with Standard Deviation	Unit
Density—fresh state	910 ± 10.04	kg/m^3
Density—hardened state	790 ± 9.43	kg/m^3
Thermal conductivity	0.1277 ± 0.0002	W/(m·K)
Sound absorption weighed/class	0.45/A	-
Compressive stress at 10% strain	782.4 ± 8.76	kPa
Shrinkage (linear)	1.85 ± 0.23	%

The determination of sorption properties was carried out through the same method as for pure hardened clay, using desiccators with solutions at a given relative humidity according to EN ISO 12571 [55]. The results are plotted in the form of sorption and desorption curves in Figure 8. The positive effect of adding natural fibers (straw fibers) into the clay matrix with regard to the sorption activity of the composite material can be observed, caused by an increase in open porosity. Based on these results, it can be concluded that the material exhibits a suitable sorption activity, making it suitable for use in indoor humidity regulation.

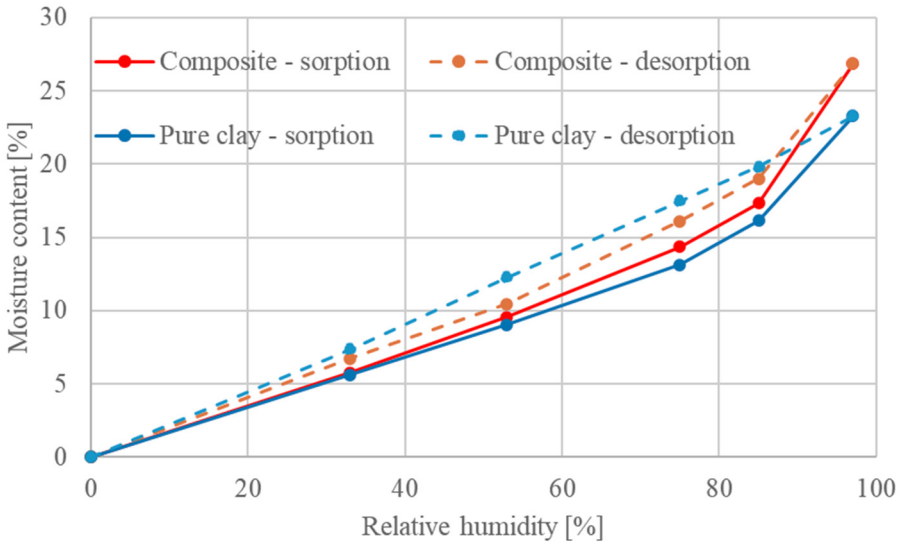

Figure 8. Sorption properties of pure clay and composite.

Furthermore, the determination of moisture adsorption as a function of time was carried out using a modified methodology. In this procedure, the samples were first exposed to an environment at 23 °C and 35% relative humidity until their weight stabilized and were then placed in an environment at 23 °C and 65% relative humidity. The change in weight was recorded at defined time intervals. The results were evaluated according to DIN 18948 [56] and are presented in Table 5.

Table 5. Evaluation of moisture buffering capacity [g/m^2].

Sample/Hours	0.5	1	3	6	9	12
Mixture (clay + straw)	18.88 ± 1.72	31.15 ± 2.42	64.23 ± 2.51	97.67 ± 1.74	128.48 ± 1.28	152.73 ± 0.75
Pure clay	27.24 ± 0.10	39.30 ± 0.34	82.56 ± 2.63	128.16 ± 4.44	169.17 ± 5.89	202.32 ± 6.99
Requirement WS III	≥6.5	≥13.0	≥26.5	≥40.0	-	≥60.0

Note: According to ISO 24 353 expression, the results are identical, only they are given in kg/m^2.

As can be seen in Table 4, all samples (composites, pure clay) can be classified as WS III (water and steam absorption class). Pure clay exhibits a higher moisture buffering capacity.

The developed clay composite had a value of the moisture buffering capacity after 12 h of 152.73 ± 0.75 g/m^2.

The moisture capacity values (MBVs) were further determined and are listed in Table 6. Since the standard cycling/conditioning of samples according to the NORDTEST methodology was not used for this experiment, the results cannot be directly classified under that standard. However, it can be assumed that the samples would fall within the excellent level. The obtained average values of the moisture buffering capacity for the composite made of clay with a higher proportion of montmorillonite and straw are very good. These values even exceed those published by Palumbo et al. [66], whose bio composite samples exhibited MBVs ranging from 2.49 to 2.73 g/ΔRV/m^2.

Table 6. Determination of average moisture capacity values [g/ΔRV/m^2].

Sample/Hours	0.5	1	3	6	9	12
Mixture (clay + straw)	0.63	1.04	2.14	3.26	4.28	5.09
Pure clay	0.91	1.31	2.75	4.27	5.64	6.74

The results were further used to determine the moisture sorption/desorption rate [kg/(m^2·h)] according to ISO 24 353 [58]. The results are presented in Table 7 and Figure 9.

Table 7. Determination of average moisture sorption/desorption rate [kg/(m^2·h)].

Sample/Hours	0.5	1	3	6	9	12
Mixture (clay + straw)	0.0378	0.0312	0.0214	0.0163	0.0143	0.0127
Pure clay	0.0545	0.0393	0.0275	0.0214	0.0188	0.0169

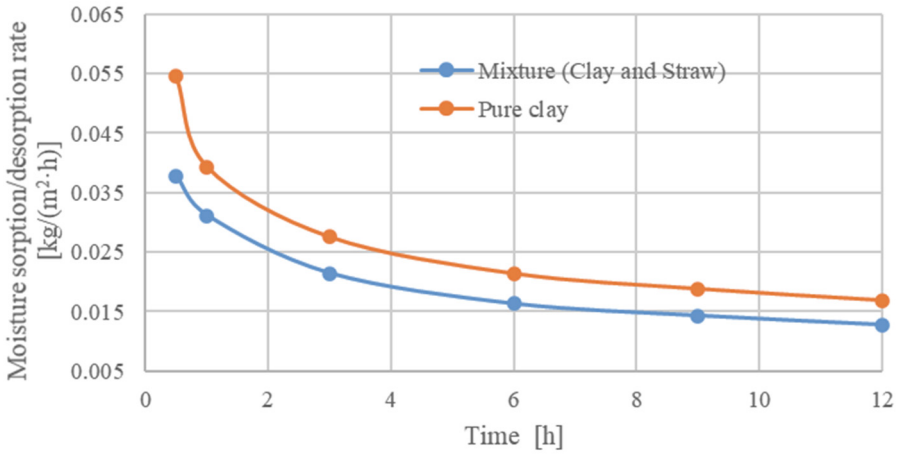

Figure 9. Moisture sorption rate.

4.5. Overview of Results Determined in Boxes (Clay Composite with Green Elements)

Next, Figures 10 and 11 show the temporal progression of relative humidity and temperature during the measurement period for *E. aureum* and *C. comosum*, respectively, with one, two and three clay plates. RH_1 and Temp_1 correspond to the measured values in the chamber without clay plates, while RH_2 and Temp_2 represent the values in the chamber with clay plates.

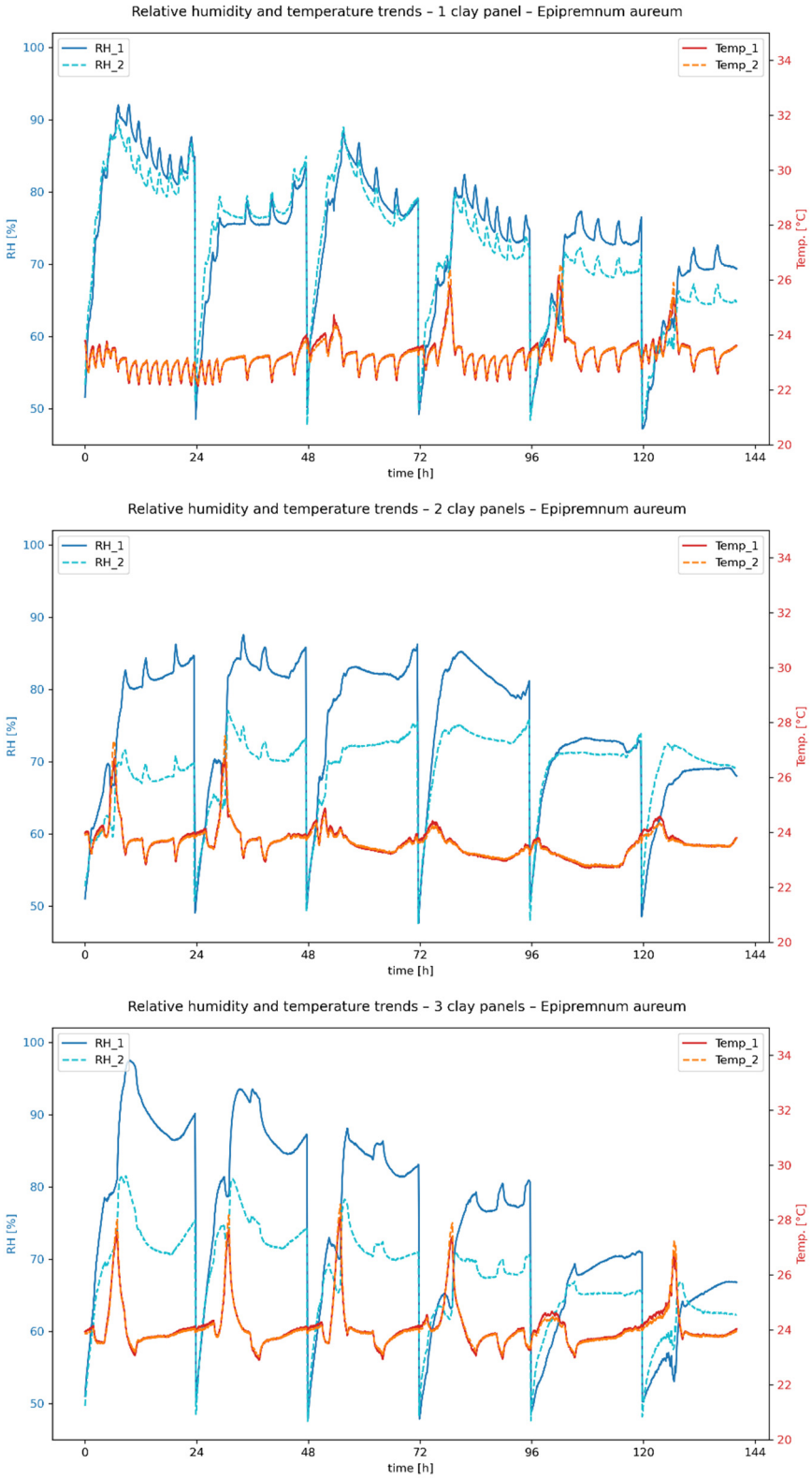

Figure 10. Relative humidity and temperature trends—*E. aureum*.

The measurements initially show clear differences in the evaporation performance of the plant species studied. In the first 48 h after the start of measurement, the average relative humidity in the reference chamber was 79.58% for *E. aureum* (ivy), while *C. comosum* (spider plant) reached a value of 84.35%. Over the entire period, the average maximum value for *E. aureum* was 92.38%, and for *C. comosum* it was 96.21%. Since the same substrate

mixtures were used for all experiments, the results indicate that *C. comosum* has a higher evaporation rate.

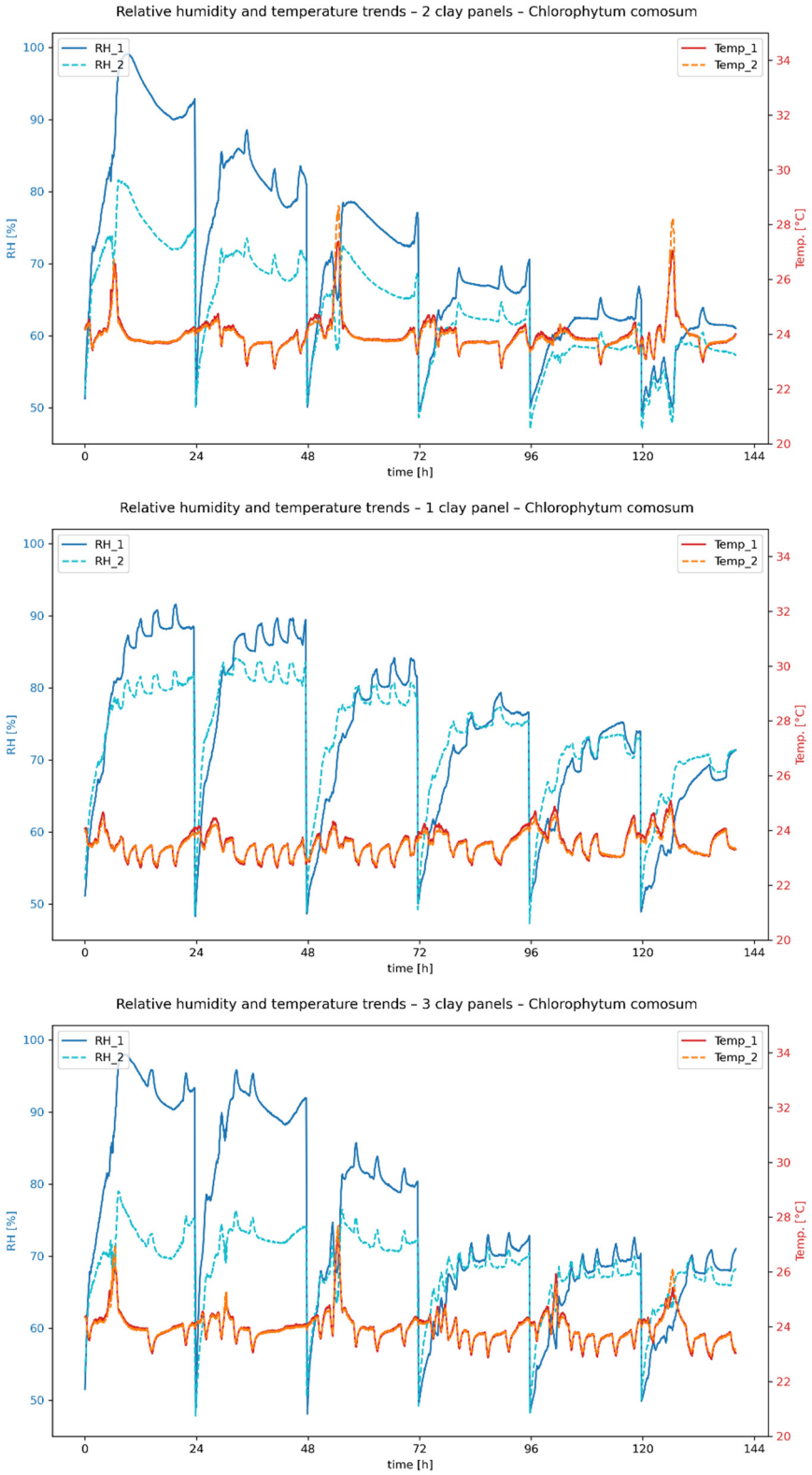

Figure 11. Relative humidity and temperature trends—*C. comosum*.

Table 8 shows the results of the ANOVA test for the humidity values in the chambers without clay plates between *C. comosum* and *E. aureum*. Since the *p*-value for the plant effect was <0.001, the null hypothesis was rejected. This shows that there are statistically

significant differences between the humidity values of the *C. comosum* and *E. aureum* in the chamber without a clay plate.

Table 8. Statistical analyses of *C. comosum* and *E. aureum*.

ANOVA-Test	f-Statistic	*p*-Value	η^2	df (Between, Within)
Plants	77.303	<0.001 (1.6×10^{-18})	0.003	(1, 25,204)

The temporal progression of humidity also supports this finding. While humidity decreases slowly in *E. aureum*, *C. comosum* shows a significantly faster decline, which could indicate a higher water consumption at the beginning. The drier substrate then leads to a comparatively more significant reduction in evaporation.

Figures 12 and 13 show the humidity difference between the reference chamber, equipped with only one plant and the chamber with additional clay plates. The difference was calculated as follows: $\text{chamber}_{\text{plant}}$—$\text{chamber}_{\text{plant+plate}}$. A clear difference in humidity was observed between the test chambers. The difference increased with the number of clay plates, with the difference between one and two plates being significantly greater than that between two and three plates (see Table 8).

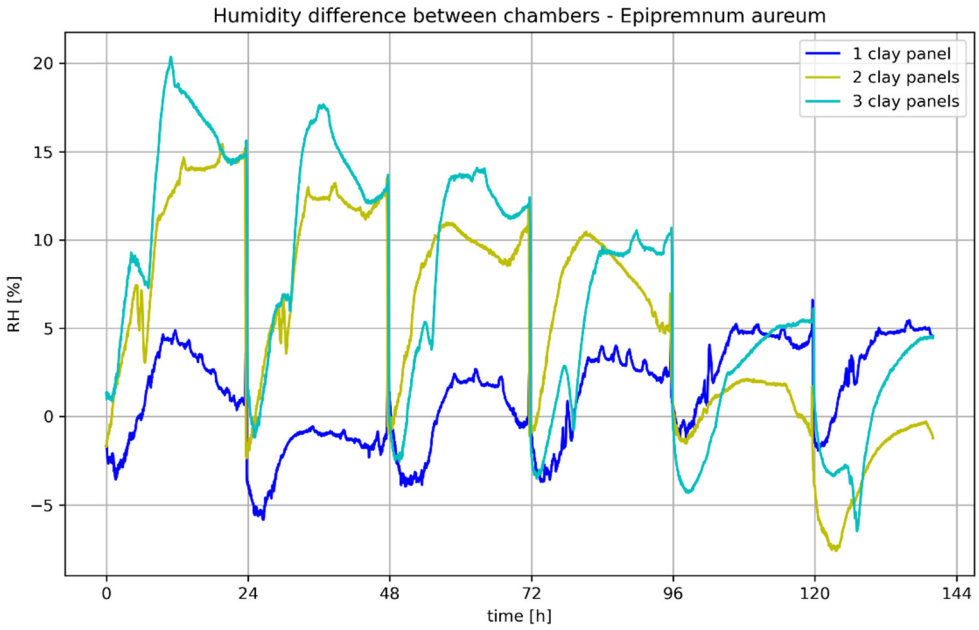

Figure 12. Humidity differences, ΔRH, between the chambers—*E. aureum*.

At the start of all experiments, there was a positive difference in air humidity, i.e., the air humidity in the chamber with clay panels was lower than in the reference chamber. This indicates that the clay panels initially absorbed moisture from the air, which is consistent with the previous results for clay panels. The absolute difference in relative humidity reached a maximum value of just under 20% RH for *E. aureum* with three clay panels, while *C. comosum* was significantly above 20% RH due to the higher initial humidity, resulting in a higher evaporation. The other maximum values are listed in Table 9. In general, it was found that the difference between the chambers increased with increasing initial air humidity.

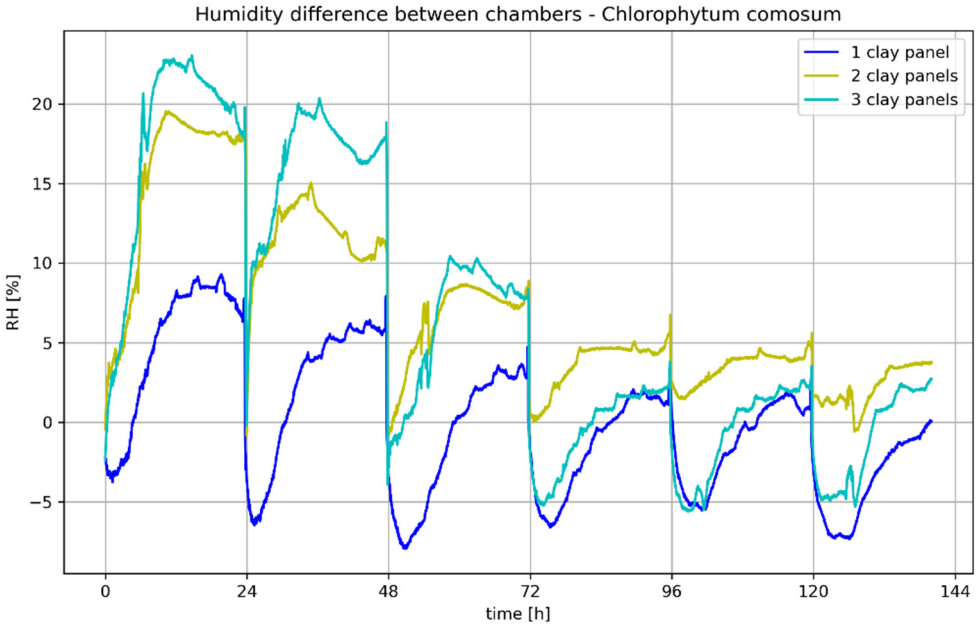

Figure 13. Humidity differences, ΔRH, between the chambers—*C. comosum*.

Table 9. Maximum difference in RH (%) between reference chamber and measuring chamber.

Plant	One Clay Plate	Two Clay Plates	Three Clay Plates
E. aureum	6.61	15.42	20.36
C. comosum	9.28	19.59	23.04

However, negative differences were also observed. These occurred immediately after the injection of dry compressed air for up to 3 h, but also over longer periods at later measurement times. Short-term negative differences can be explained by the short-term evaporation of the clay panels when low humidity is blown in, which means that the increase in humidity in the chamber with clay panels was slower than in the reference chamber after the humidity was reduced. Longer negative phases are probably related to the saturation of the clay panels and the evaporation capacity of the plants. As shown in Figure 9, the boards can store a limited amount of water depending on the air humidity. If the air humidity drops as a result of the introduction of compressed air, desorption or evaporation occurs, especially at low air humidities and evaporation rates of the plants. This effect is particularly evident in the experiments with only one clay plate, which releases moisture into the ambient air from the second day of measurement onwards. With several clay plates, this phenomenon shifts further towards the end of the measurement due to the larger storage mass.

In general, the difference between the air humidity levels during the desorption of the clay plates is significantly lower than the absorption at high air humidity levels. However, it is to be expected that the desorption rate will continue to increase at even lower air humidity levels.

The weight of the clay plates at the end of the measurement was higher than the initial weight in all test series. The evaluation shows that the difference between the initial and final weights consistently depends on the final humidity: the higher the final humidity, the greater the weight gain of the clay plates. On average, the weight gain compared to the conditioned clay plate was 1.02% or 2.28 g, with a maximum of 1.71% or 3.75 g at a high final moisture content of 69.02% in the chamber with clay slab and a minimum of 0.45% or 1.05 g at a low final moisture content of 57.26%.

5. Conclusions

The aim of the research was to study the moisture behavior of environmentally friendly, natural composites based on clay and natural fibers, including the study of their interaction with green elements, which represent a unique and ecological solution to the problem of unsuitable indoor conditions. The goal was to design a sorption-active material that would improve indoor microclimatic conditions, such as regulating relative humidity and possibly other parameters of the indoor environment. In practice, this material should be complemented with green elements that serve as an additional source of moisture where indoor humidity is insufficient and therefore unsuitable for maintaining a healthy environment.

For the development of this material, clay with a higher proportion of montmorillonite was used. Due to its crystallography, it is able to bind a larger amount of water molecules into its structure compared to, e.g., kaolinitic or illitic clays. This behavior was confirmed in the conducted and published work. However, montmorillonite clay exhibits high volume changes when moisture content changes. Montmorillonite clay showed a shrinkage of approximately 14.81% and also contained a large amount of mixing water, as the w_{opt} reached a value of 50.6%, which is approximately double the optimum moisture content exhibited, for example, by brickmaking clays, where the optimum moisture content is usually in the range of 20–25%. Therefore, a natural fibrous binder from agriculture was added to this clay to eliminate this effect.

Based on the results obtained in this experiment, it can be stated that the resulting composite exhibits good basic physical, acoustic and thermal insulation properties, especially with regard to interior cladding elements. It was confirmed that adding fibers to the clay matrix leads to a slight increase in open porosity, as well as a reduction in bulk density, which leads to an improvement in thermal insulation and sorption properties. In the case of this type of clay, which is highly sensitive to drying, the addition of natural fibers leads to a substantial reduction in the shrinkage. The addition of a natural filler reduced shrinkage from 14.81% to just 1.85%, i.e., by approximately 87.5% overall. This should significantly contribute to the manufacturability of, for example, cladding elements made from this composite in larger dimensions and significantly reduce the complexity of production in the area of drying.

Based on the study of moisture behavior, the developed clay composite can be classified as class WSIII (water and steam absorption class) according to DIN 18948, with a moisture buffering capacity of 152.73 g/m^2 after 12 h. The evaluation of the moisture buffering capacity indicated that the samples of the developed mixture would be classified as "excellent" according to NORDTEST methodology (even considering the modified testing approach), as the moisture buffering capacity after 8 h exceeded 2 $g/\Delta RV/m^2$.

Overall, it can be stated that the final composite exhibits similar properties, including sorption capacity and other parameters in terms of moisture sorption rate, to those of pure clay and significantly higher than those of materials made from common types of clay containing a predominant proportion of illite or kaolinite. In this case, however, it is also necessary to take into account the fact that the parameters are given in kg/m^2 (g/m^2) and the sorption properties are given in % by weight. When converted to volumetric moisture, the sorption capacity is even higher overall.

A small-scale experiment was conducted to verify the effectiveness of the moisture regulation of these environmentally friendly clay composites in combination with green elements (*E. aureum*, *C. comosum*). The results confirmed the potential of clay composites as short-term humidity regulators. Regarding the plants used, the variant combining *C. comosum* with two or three composite plates performed better. In Figures 10–13, it is evident that composite materials are able to sorb moisture and limit the negative increase in humidity in the space where there is a significant moisture source. This fact is evident

especially from the first cycles, where the greatest effect of composites placed in chambers is evident. This effect logically subsequently decreases with the decreasing moisture content in the boxes, which is always pushed out of the chambers partially after 24 h by compressed dry air. The maximum difference in relative humidity between the reference chamber and the chamber containing both *C. comosum* and clay plates was measured at 23.04%.

In conclusion, it can be stated that these developed elements could serve as indoor cladding elements in synergy with green elements that will ideally regulate the microclimatic conditions of the interior, especially as a solution for short-term humidity changes in the interior, e.g., bedrooms and bathrooms. Their good thermal insulation and acoustic properties would also be an added value for the interior.

Author Contributions: Conceptualization, J.P. and J.Z.; methodology, J.P., J.Z. and A.K.; formal analysis, J.P., J.Z. and A.K.; investigation, J.P. and J.Z.; resources, J.P. and V.N.; data curation, J.P., V.N., A.K., A.S. and J.O.S.; writing—original draft preparation, J.P., J.Z., A.K. and J.O.S.; writing—review and editing, J.P. and J.O.S.; visualization, J.P., V.N. and A.S.; supervision, J.P., J.Z. and A.K.; project administration, J.P. and A.K.; funding acquisition, J.P. and A.K. All authors have read and agreed to the published version of the manuscript.

Funding: This paper was elaborated and funded within the bilateral research project between the Czech Republic and Austria (Czech Science Foundation: 23-06542K, Austrian Science Fund (FWF): 10.55776/I6398) "Study of the hygroaccumulative effect of natural based materials and their influence on the moisture stability of the indoor environment of buildings". For open access purposes, the author has applied a CC BY public copyright license to any author-accepted manuscript version arising from this submission (https://creativecommons.org/licenses/by/4.0/, accessed on 30 September 2025).

Data Availability Statement: The original contributions presented in the study are included in the article; further inquiries can be directed to the corresponding author.

Conflicts of Interest: The authors declare no conflicts of interest.

Abbreviations

The following abbreviations are used in this manuscript:

MBV	Moisture Buffer Value
RH	Relative Humidity
SDB	Sensitivity to Drying
SEM	Scanning Electron Microscope
WS	Water and Steam Absorption Class
XRD	X-ray Diffraction Analysis

References

1. Posch, J. Gesund Bauen. Gesund Leben. In *Wissenschaftliche Erkenntnisse über die Wirkungsweise von Baustoffen aus dem Viva Forschungspark*; Viva Research Park: Wopfing, Austria, 2018.
2. Randazzo, L.; Montana, G.; Hein, A.; Castiglia, A.; Rodonò, G.; Donato, D.I. Moisture absorption, thermal conductivity and noise mitigation of clay based plasters: The influence of mineralogical and textural characteristics. *Appl. Clay Sci.* **2016**, *132–133*, 498–507. [CrossRef]
3. Ashour, T.; Wieland, H.; Georg, H.; Bockisch, F.J.; Wu, W. The influence of natural reinforcement fibres on insulation values of earth plaster for straw bale buildings. *Mater. Des.* **2010**, *31*, 4676–4685. [CrossRef]
4. Houben, H.; Doat, P.; Schroeder, H. *Earth Construction: A Comprehensive Guide*; CRATerre-EAG & The UNESCO Chair Earthen Architecture: Grenoble, France, 2023; ISBN 978-2-86905-030-2.
5. Hu, Z.; Jeanmairet, G.; Sorella, S. Toward accurate adsorption energetics on clay surfaces: The interplay of van der Waals and quantum Monte Carlo interactions. *J. Chem. Phys.* **2016**, *145*, 194703. [CrossRef]
6. Jeanmairet, G.; Levesque, M.; Borgis, D. Hydration of clays at the molecular scale: The promising perspective of classical density functional theory. *J. Mol. Liq.* **2014**, *212*, 71–76. [CrossRef]

7. Pollak, H.; Rulíšek, S.; Pestov, A. Modeling Realistic Clay Systems with ClayCode. *J. Chem. Theory Comput.* **2024**, *20*, 2345–2358. [CrossRef] [PubMed]
8. Psotová, B. Determination of Sorption Properties of Alumina Materials. Diploma Thesis, Mendel University in Brno, Brno, Czech Republic, 2016.
9. Zhao, L.; Deng, A.; Hong, H.; Zhao, J.; Algeo, T.J.; Liu, F.; Luozhui, N.; Fang, Q. Unraveling clay-mineral genesis and climate change on Earth and Mars using machine learning-based VNIR spectral modelling. *Am. Mineral.* **2025**, *110*, 217–231. [CrossRef]
10. Nzeukou, A.N.; Tsozué, D.; Bomeni, I.Y.; Mache, J.R.; Kwopnang, M.R.; Fagel, N. Clay mineralogy in mylonite weathering products from Njimom (west Cameroon): Origin and terracotta suitability. *Disc. Geosc.* **2024**, *2*, 69. [CrossRef]
11. Skipper, N.T.; Sposito, G.; Sutton, R. Hydration and swelling of smectite clays: A computer simulation study. *Clay Miner.* **2006**, *41*, 671–678.
12. Peterková, J.; Zach, J.; Novák, V.; Korjenic, A.; Sulejmanovski, A.; Sesto, E. Optimizing Indoor Microclimate and Thermal Comfort Through Sorptive Active Elements: Stabilizing Humidity for Healthier Living Spaces. *Buildings* **2024**, *14*, 3836. [CrossRef]
13. Farrokhrouz, M.; Asef, M.R. *Shale Engineering: Mechanics and Mechanisms*, 1st ed.; CRC Press: Boca Raton, FL, USA, 2013; ISBN 9780415874199.
14. Sposito, G. *The Chemistry of Soils*, 3rd ed.; Oxford University Press: Oxford, UK, 2016; ISBN 9780190630881.
15. Madejová, J.; Komadel, P. FTIR study of structural OH groups in smectites. *Clays Clay Miner.* **2001**, *49*, 410–432. [CrossRef]
16. Kittnerová, J. Clay Plasters with Natural Additives: Transport Properties, Sorption and Durability. Ph.D. Thesis, Czech Technical University in Prague, Prague, Czech Republic, 2022.
17. Lima, J.; Faria, P.; Silva, A.S. Earth Plasters: The Influence of Clay Mineralogy in the Plasters' Properties. *Int. J. Archit. Herit.* **2020**, *14*, 948–963. [CrossRef]
18. Altmäe, E.; Ruus, A.; Raamets, J.; Tungel, E.; Johansson, D.; Bagge, H.; Wahlstrom, A. Determination of Clay-Sand Plaster Hygrothermal Performance: Influence of Different Types of Clays on Sorption and Water Vapour Permeability. In *Springer Proceedings in Energy: Cold Climate HVAC 2018: Sustainable Buildings in Cold Climates*; Springer: Cham, Switzerland, 2019; pp. 945–955. [CrossRef]
19. Ghavami, K.; Toledo Filho, R.D.; Barbosa, N.P. Behaviour of composite soil reinforced with natural fibres. *Cem. Concr. Compos.* **1999**, *21*, 39–48. [CrossRef]
20. Mohamed, A.E.M.K. Improvement of swelling clay properties using hay fibers. *Constr. Build. Mater.* **2013**, *38*, 242–247. [CrossRef]
21. Bouhicha, M.; Aouissi, F.; Kenai, S. Performance of composite soil reinforced with barley straw. *Cem. Concr. Compos.* **2005**, *27*, 617–621. [CrossRef]
22. Hamard, E.; Morel, J.-C.; Salgado, F.; Marcom, A.; Meunier, N. A procedure to assess the suitability of plaster to protect vernacular earthen architecture. *J. Cult. Herit.* **2013**, *14*, 109–115. [CrossRef]
23. Meglio, E.; Formisano, A. Experimental Tests on Hemp-Reinforced Adobe Bricks. In *Lecture Notes in Civil Engineering, Proceedings of the Conference Paper—5th International Conference on Protection of Historical Constructions, PROHITECH 2025, Naples, Italy, 26–28 March 2025*; Springer: Cham, Switzerland, 2025; pp. 197–204.
24. Hurtado-Figueroa, O.; Varum, H.; Prieto, M.I.; Amaya, R.J.G.; Escamilla, A.C. Effect of fiber-matrix interaction and embedment length on the pullout behavior of rice straw fibers embedded in clay matrix. *Results Eng.* **2025**, *27*, 106144. [CrossRef]
25. Koutous, A.; Hilali, E. Reinforcing rammed earth with plant fibers: A case study. *Case Stud. Constr. Mat.* **2021**, *14*, e00514. [CrossRef]
26. Liuzzi, S.; Rubino, C.; Martellotta, F. Properties of clay plasters with olive fibers. In *Bio-Based Materials and Biotechnologies for Eco-Efficient Construction*; Woodhead Publishing: Cambridge, UK, 2020; pp. 171–186. [CrossRef]
27. Liuzzi, S.; Rubino, C.; Stefanizzi, P.; Petrella, A.; Boghetich, A.; Casavola, C.; Pappalettera, G. Hygrothermal properties of clayey plasters with olive fibers. *Constr. Build. Mat.* **2018**, *158*, 24–32. [CrossRef]
28. Laborel-Préneron, A.; Aubert, J.E.; Magniont, C.; Tribout, C.; Bertron, A. Plant aggregates and fibers in earth construction materials: A review. *Constr. Build. Mat.* **2016**, *111*, 719–734. [CrossRef]
29. Swearingen, C.; Macha, S.; Fitch, A. Leashed ferrocenes at clay surfaces: Potential applications for environmental catalysis. *J. Molec. Cat. A Chem.* **2003**, *199*, 149–160. [CrossRef]
30. Darling, E.K.; Corsi, R.L. Field-to-laboratory analysis of clay wall coatings as passive removal materials for ozone in buildings. *Indoor Air.* **2017**, *27*, 3. [CrossRef]
31. Darling, E.K.; Corsi, R.L. Passive removal materials for indoor ozone control. *Build. Environ.* **2016**, *106*, 33–44. [CrossRef]
32. Darling, E.K.; Cros, C.J.; Wargocki, P.; Kolarik, J.; Morrison, G.C.; Corsi, R.L. Impacts of a clay plaster on indoor air quality assessed using chemical and sensory measurements. *Build. Environ.* **2012**, *57*, 370–376. [CrossRef]
33. Hu, C.; Teng, F.; Yin, X.; Wang, P.; He, B.; Zhu, L. Adsorption of heavy metals using cysteine-modified pillared montmorillonite: Mechanisms and characteristics. *Appl. Clay Sci.* **2025**, *276*, 107923. [CrossRef]

34. Kausor, M.A.; Gupta, S.S.; Bhattacharyya, K.G.; Chakrabortty, D. Montmorillonite and modified montmorillonite as adsorbents for removal of water soluble organic dyes: A review on current status of the art. *Inorg. Chem. Commun.* **2022**, *143*, 109686. [CrossRef]
35. *EN 15665*; Ventilation for buildings—Determining Performance Criteria for Residential Ventilation Systems. CEN-CENELEC Management Centre: Brussels, Belgium, 2009.
36. *EN 16798-1*; Energy Performance of Buildings—Ventilation for Buildings—Part 1: Indoor Environmental Input Parameters for Design and Assessment of Energy Performance of Buildings Addressing Indoor Air Quality, Thermal Environment, Lighting and Acoustics—Module M1-6. CEN-CENELEC Management Centre: Brussels, Belgium, 2019.
37. Andadari, T.S.; Satwiko, P.; Purwanto, L.; Soesilo, R. Methods, Area Ratio and Plants of Biowall to Induce Atmospheric Comfort: A Review. *J. Sustain. Archit. Civ. Eng.* **2024**, *35*, 2. [CrossRef]
38. Wang, C.; Hu, Q.; Zhou, Z.; Li, D.; Wu, L. Adding Green to Architectures: Empirical Research Based on Indoor Vertical Greening of the Emotional Promotion on Adolescents. *Buildings* **2024**, *14*, 2251. [CrossRef]
39. Peterková, J.; Michalčíková, M.; Novák, V.; Slávik, R.; Zach, J.; Korjenic, A.; Hodná, J.; Raich, B. The influence of green walls on interior climate conditions and human health. In Proceedings of the 4th Central European Symposium on Building Physics (CESBP 2019), MATEC Web of Conferences, Prague, Czech Republic, 2–5 September 2019; EDP Sciences: Les Ulis, Francie, 2019; pp. 1–7, ISSN 2261–236X.
40. Davis, M.J.M.; Tenpierik, M.J.; Ramírez, F.R.; Pérez, M.E. More than just a Green Facade: The sound absorption properties of a vertical garden with and without plants. *Build. Environ.* **2017**, *116*, 64–72. [CrossRef]
41. Azkorra, Z.; Pérez, G.; Coma, J.; Cabeza, L.F.; Burés, S.; Álvaro, J.E.; Erkoreka, A.; Urrestarazu, M. Evaluation of green walls as a passive acoustic insulation system for buildings. *Appl. Acoust.* **2015**, *89*, 46–56. [CrossRef]
42. Peterková, J.; Zach, J.; Michalčíková, M.; Novák, V.; Slávik, R.; Donaťáková, D.; Korjenic, A.; Raich, B. Healthy Solutions for Interior Acoustics Using Green Elements. *TZB-info* **2019**, *44*, 1–12. Available online: https://stavba.tzb-info.cz/akustika-staveb/19776-zdrave-reseni-akustiky-interieru-pomoci-zelenych-prvku?utm_source=newsletter&utm_medium=email&utm_campaign=Newsletter_2019-10-29 (accessed on 15 August 2025).
43. Van Renterghem, T. Towards explaining the positive effect of vegetation on the perception of environmental noise. *Urb. Forest. Urb. Green.* **2018**, *40*, 133–144. [CrossRef]
44. *ÖNORM L 1133*; Interior landscaping—Planning, Execution and Maintenance. Austrian Standards Institute: Vienna, Austria, 2017.
45. Pavlová, L. Plant Physiology. 2006. Available online: https://kfrserver.natur.cuni.cz/studium/prednasky/pavlova/fyzrost/3_Fotosynteza.pdf (accessed on 20 September 2025).
46. *EN ISO 12 677*; Chemical Analysis of Refractory Products by X-Ray Fluorescence (XRF)—Fused Cast-Bead Method. Czech Agency for Standardization: Prague, Czech Republic, 2012.
47. *EN 1097-3*; Tests for Mechanical and Physical Properties of Aggregates—Part 3: Determination of Loose Bulk Density and Voids. CEN-CENELEC Management Centre: Brussels, Belgium, 1998.
48. *EN 933-2*; Tests for Geometrical Properties of Aggregates—Part 2: Determination of Particle Size Distribution—Test Sieves, Nominal Size of Apertures. CEN-CENELEC Management Centre: Brussels, Belgium, 2020.
49. *CSN 72 1074*; Determination of Optimum and Processing Moisture of Ceramic Masses by Means of Pfefferkorn Apparatus. Czech Agency for Standardization: Prague, Czech Republic, 2015.
50. *CSN 72 1073*; Determination of Change in Length of Ceramic Materials by Drying and Calcining. Czech Agency for Standardization: Prague, Czech Republic, 2015.
51. *CSN 722603*; Testing of Brick Products. Determination of Mass, Volume Mass and Absorptivity. Czech Standardization Institute: Prague, Czech Republic, 1979.
52. *EN ISO 29470*; Thermal Insulating Products for Building Applications—Determination of the Apparent Density. CEN-CENELEC Management Centre: Brussels, Belgium, 2020.
53. *CSN 721565-7*; Testing of Brick Clays. Determination of the Transverse Strength. Czech Agency for Standardization: Prague, Czech Republic, 1986.
54. *EN ISO 29469*; Thermal Insulating Products for Building Applications—Determination of Compression Behaviour. CEN-CENELEC Management Centre: Brussels, Belgium, 2022.
55. *EN ISO 12571*; Hygrothermal Performance of Building Materials and Products—Determination of Hygroscopic Sorption Properties. CEN-CENELEC Management Centre: Brussels, Belgium, 2021.
56. *DIN 18948*; Earthen Boards—Requirements, Test and Labelling. German Institute for Standardisation: Berlin, Germany, 2024.
57. Rode, C.; Peuhkuri, R.H.; Hansen, K.K.; Time, B.; Svennberg, K.; Arfvidsson, J.; Ojanen, T. NORDTEST Project on Moisture Buffer Value of Materials. In Proceedings of the AIVC 26th Conference: Ventilation in Relation to the Energy Performance of Buildings, Air Infiltration and Ventilation, Bruxelles, Belgium, 21–23 September 2005; pp. 47–52.

58. *ISO 24353*; Hygrothermal Performance of Building Materials and Products—Determination of Moisture Adsorption/Desorption Properties in Response to Humidity Variation. International Organization for Standardization: Geneva, Switzerland, 2008.
59. *ISO 10534-1*; Acoustics—Determination of Sound Absorption Coefficient and Impedance in Impedance Tubes—Part 1: Method Using Standing Wave Ratio. International Organization for Standardization: Geneva, Switzerland, 1996.
60. *EN ISO 11654*; Acoustics—Sound Absorbers for Use in Buildings—Rating of Sound Absorption. International Organization for Standardization: Geneva, Switzerland, 1997.
61. Streit, E.; Schabauer, J.; Korjenic, A. Evaluating Particulate Matter Reduction by Indoor Plants in a Recirculating Air System. *Atmosphere* **2025**, *16*, 783. [CrossRef]
62. *DIN ISO 3310-1*; Test Sieves—Technical Requirements and Testing—Part 1: Test Sieves of Metal Wire Cloth. German Institute for Standardisation: Berlin, Germany, 2001.
63. *ISO 565*; Test Sieves. Metal Wire Cloth, Performated Metal and Electroformed Sheet. Nominal Size of Openings. International Organization for Standardization: Geneva, Switzerland, 1990.
64. *EN 12524*; Building Materials and Products—Hygrothermal Properties—Tabulated Design Values. Czech Agency for Standardization: Prague, Czech Republic, 2001.
65. Bošková, D.; Kulhánek, F. *Building Physics II: Building Thermal Engineering*; Czech Technical University: Prague, Czech Republic, 2015; ISBN 978-80-01-05645-5.
66. Palumbo, M.; McGregor, F.; Heath, A.; Walker, P. The influence of two crop by-products on the hygrothermal properties of earth plasters. *Build. Environ.* **2016**, *105*, 245–252. [CrossRef]